

# Sensitivity enhancement for colorimetric glucose assays on whole blood by on-chip beam-guidance

M. Grumann · J. Steigert · L. Riegger · I. Moser ·  
B. Enderle · K. Riebeseel · G. Urban · R. Zengerle ·  
J. Ducr e

Published online: 27 May 2006  
© Springer Science + Business Media, LLC 2006

**Abstract** In this paper, we present a novel concept for optical beam-guidance to significantly enhance the sensitivity of colorimetric assays by extending the optical path length through the detection cell which linearly impacts the resulting attenuation of a probe beam according to the law of Beer-Lambert. In our setup, the incident probe beam is deflected by 90° into the chip plane at monolithically integrated V-grooves to pass a flat detection cell at its full width (*i.e.*, with a path length of 10 mm) instead of its usually much smaller height. Afterwards, the attenuated beam is redirected by another V-groove towards an external detector. The general beam-guidance concept is demonstrated by a glucose assay on human whole blood on a centrifugal microfluidic “lab-on-a-disk” platform made of COC. We achieve an excellent linearity with a correlation coefficient ( $R^2$ ) of 0.997 paired with a lower limit of detection (200  $\mu\text{M}$ ) and a good reproducibility with a coefficient of variation ( $CV$ ) of 4.0% over nearly three orders of magnitude. With an accelerated sedimentation of cellular constituents by centrifugal forces, the sample of whole blood can be analyzed in a fully integrated fashion within 210 s. This time-to-result can even be improved by the numerical extrapolation of the saturation value. Additionally, the direct assay on whole blood also shows a negligible correlation with the hematocrit of the blood sample.

**Keywords** Glucose · Optical beam-guidance · Lab-on-a-disk · Colorimetric assay · Total internal reflection

## Introduction

For many years, numerous approaches have been reported to transfer clinical diagnostics to miniaturized point-of-care applications. So-called “lab-on-a-chip” or “micro total analysis systems” ( $\mu\text{TAS}$ ) are addressed to meet the special requirements such as full process integration, reproducibility, reduced consumption of sample and reagents, short times-to-result, and ease of handling (Oosterbroek and van den Berg, 2003; Vilkner et al., 2004; Sia et al., 2004; Schulte et al., 2002; Ducr e and Zengerle, 2004; Reyes et al., 2002; Auroux et al., 2002). The multitude of commercially available devices (Examples in clinical diagnostics, 2004) corroborates the economic prospects which are widely attributed to lab-on-a-chip technologies.

Apart from the integration of preparative steps, a highly accurate, robust and possibly “low-cost” detection method is required. Besides electrochemical methods, optical detection has been widely used (Verpoorte, 2003). In particular, for routine diagnostics, absorption measurements have been the method of choice and a multitude of colorimetric assays have been developed for the easily accessible visible range. The intensity of the signal generally depends on the optical path length through the medium and on the decrease in signal intensity induced by the colored product of an indicator. In miniaturized formats, the sensitivity suffers from the significantly reduced optical path lengths compared to macroscopic setups. To extend the path length for a typically perpendicular incidence of a probe beam, optical waveguides (Verpoorte et al., 1992; Splawn and

M. Grumann (✉) · J. Steigert · L. Riegger · R. Zengerle · J. Ducr e  
Lab for MEMS Applications, IMTEK—University of Freiburg,  
Georges-Koehler-Allee 106, 79110 Freiburg, Germany  
e-mail: grumann@imtek.de

I. Moser · B. Enderle · K. Riebeseel · G. Urban  
Lab for Sensors, IMTEK—University of Freiburg,  
Georges-Koehler-Allee 106, D-79110 Freiburg, Germany

Lytle, 2002), microlenses (Roulet et al., 2001), or optical fibers (Liang et al., 1996; Petersen et al., 2002) are integrated on flat microfluidic chips accommodating low-aspect-ratio detection cells (Walt, 2000). However, these approaches require rather complex chip designs and an elaborate, high-accuracy alignment of the optical components.

In our work, optical beam-guidance to extend the path length of a probe beam is achieved by total internal reflection (TIR) at monolithically integrated V-grooves (Grumann et al.). This novel optical method is experimentally validated by a common, enzymatically catalyzed glucose assay on human whole blood. A first enzyme oxidizes the glucose and a second enzyme converts a reagent to a colored product. The formation of this product increases the optical absorbance at a specific wavelength, thereby indicating the initial glucose concentration.

For the technical implementation, we use centrifugal microfluidic technologies (Madou and Kellogg, 1998; Madou et al., 2000; Ekstrand et al., 2000; Badr et al., 2002; Lai et al., 2004). Upon spinning, the centrifugal force transports samples and reagents from inlets near the center of disk-based channels towards the outer perimeter. The same centrifugal force also speeds up the sedimentation of suspended particles (*e.g.*, cellular constituents in whole blood).

The paper is structured in the following way. First, we introduce the optical principle and the corresponding technical implementation. Subsequently, the assay protocol is detailed and the enhancement of the sensor resolution is investigated. Next, a new, disk-based real-time method to reduce the measurement time and to provide the means for internal calibration is presented. Finally, the correlation of the measured glucose concentration on the hematocrit is studied.

## Optical concept

Colorimetric assays are based on the measurement of the intensity  $I$  of a probe beam, with an initial intensity  $I_0$ , after passing through the detection cell containing the reacted sample solution. According to the law of Beer-Lambert, the absorbance (or optical density)

$$A \equiv -\log \frac{I}{I_0} = c \cdot \varepsilon \cdot l_{\text{abs}} \quad (1)$$

linearly depends on the concentration of the analyte  $c$ , the molar extinction coefficient  $\varepsilon$  of the colored indicator, and the optical path length  $l_{\text{abs}}$  through the detection cell.

In our novel approach, the optical beam-guidance is based on total internal reflection (TIR) governed by Snell's law which occurs at the interface of the polymer substrate and air.

Assuming a refractive index of  $n_{\text{polymer}} = 1.5$  for polymers such as COC (Cyclic olefin copolymer, 2004) (cyclic olefin copolymer) or PMMA (polymethyl methacrylate) which are materials typically used in clinical diagnostics, the critical angle for TIR

$$\alpha_c = \sin^{-1} \left( \frac{n_{\text{air}}}{n_{\text{polymer}}} \right) \quad (2)$$

is exceeded for an incidence angle  $\alpha \geq 41^\circ$ . To experimentally realize this TIR-based principle (*i.e.*, to deflect the incident beam by  $90^\circ$  into the chip-plane), we engrave triangular V-grooves as reflectors with the use of a standard tapered milling head by CNC (computer numerically controlled) micromachining without additional reflective coating. The V-grooves feature a side facet angle of  $45^\circ$  at the bottom side of the flat chip (Fig. 1). This way, an optical beam impinging at  $\alpha = 45^\circ$  on the surface of the V-groove is deflected by an overall angle of  $90^\circ$  from the direction of incidence. The achieved surface roughness of the V-grooves has proven to be sufficiently low in a way that fluctuations of the assay result by varied V-grooves have been negligible. Possibly generated straylight is effectively blocked off at the circular entrance optics (Fiber Collimation Package) of the detector 10 cm above the disk.

Absorption thus takes place along the full length  $l_{\text{abs}}$  of the typically low-aspect-ratio detection cell instead of the much smaller thickness of the device for direct perpendicular incidence where the light source, detection cell, and detector are linearly arranged.

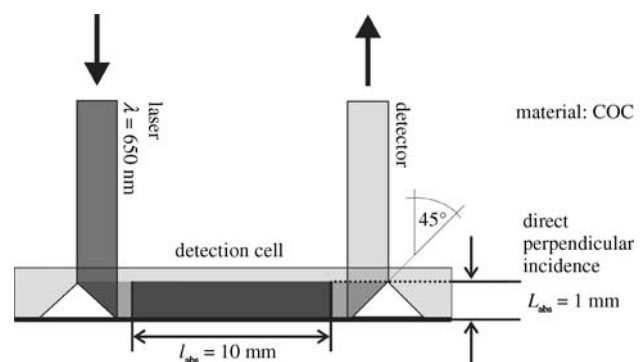


**Fig. 1** On-chip optical beam-guidance by total-internal-reflection (TIR) at monolithically integrated V-grooves at the rear side (*i.e.*, side opposite to laser and detector) of the chip. These V-grooves are inclined at  $45^\circ$  with respect to the chip surface. According to Snell's law (Eq. (2)), TIR takes place at an incident angle of  $45^\circ$  on the polymer surface, *i.e.* the probe beam impinging perpendicular on the upper chip surface is deflected by an overall angle of  $90^\circ$  into the plane of the chip. The path length  $l_{\text{abs}} = 10$  mm is thus extended by a factor of 10 compared to  $L_{\text{abs}} = 1$  mm for direct incidence

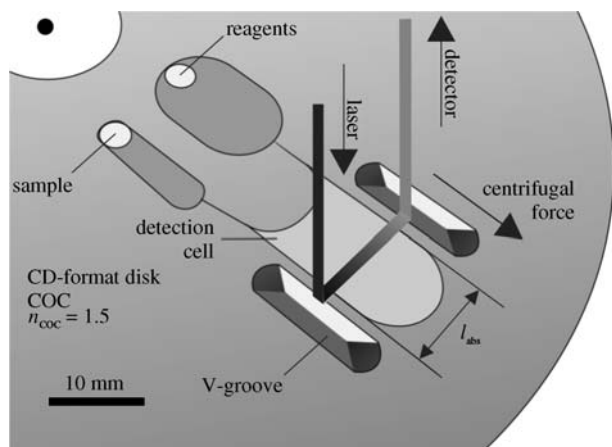


**Fig. 2** TIR-enhanced colorimetric assays implemented on a lab-on-a-disk. The COC disk, with the format of a compact disc (CD), features inlet reservoirs for sample and reagents which are connected to the detection cell ( $V_{\text{cell}} = 100 \mu\text{l}$ ). V-grooves aligned to the site of the entrance and the exit of the optical probe beam deflect the beam by TIR (Eq. (2)) perpendicularly into and out of the disk-plane towards the detector through a path length  $l_{\text{abs}}$  of 10 mm

### Implementation on-disk and experimental setup

To demonstrate both the simplicity and performance of this novel concept, a lab-on-a-disk is developed to perform a glucose assay on human whole blood. The disk, with the format of a conventional compact disc (CD), is made of COC and is manufactured by standard CNC micromachining. In addition to the optical components for beam-guidance, the disk features microfluidic structures for sample and reagent delivery as well as a cell where the reaction takes place (Fig. 2).

Two inlet reservoirs for the uptake of the sample and the reagents are connected to a detection cell with a volume of  $V_{\text{cell}} = 100 \mu\text{l}$  via hydrophobic valves (*i.e.*, hydrophobically coated geometrical constrictions) (McNeely et al., 1999; Zeng et al., 2000). At these constrictions, the channel walls are coated with Teflon to constitute a hydrophobic zone whereas the resulting capillary back pressure is further elevated by reducing the channel cross section. As a result, a centrifugally driven flow is stopped up to a critical capillary burst frequency  $\nu_c$ . Upon exceeding  $\nu_c$ , the liquids are then transported into the detection cell where mixing and the readout takes place. Next to the detection cell, V-grooves are positioned to deflect the probe beam ( $\lambda_{\text{peak}} = 650 \text{ nm}$ ) of a standard laser diode (Laserdiode, 2004) into the chip plane and, after the probe beam has been attenuated in the detection cell, out of the chip towards an external spectrophotometer (UV/VIS Microspectrometer, 2004). In contrast to commonly used photodiodes in this field of application, the applied spectrophotometer is able to discriminate colors. This feature allows running a wide range of colorimetric as-

says at different probe wavelengths (Grumann et al., 2005c) from different lasers. Even fluorescence immunoassays (FIA) (Grumann et al., 2005d) are compatible to this readout device.

### Assay protocol

The glucose concentration in human whole blood is determined colorimetrically in a two-step enzymatic reaction. First,  $30 \mu\text{l}$  of a 1:100 dilution of the blood sample with PBS buffer (Phosphate buffered saline—PBS) is loaded into the disk and mixed with the reagents ( $V_{\text{reagents}} = 70 \mu\text{l}$ ). These reagents are glucose oxidase (GOD)(GOD, 2005), horseradish peroxidase (HRP)(HRP, 2005), and 2,2'-Azino-bis(3-ethylbenzthiazoline-6-sulfonic acid (ABTS)(ABTS, 2005) as indicator. In the presence of  $\text{O}_2$ , GOD catalyzes the oxidation of glucose while producing stoichiometric amounts of hydrogen peroxide ( $\text{H}_2\text{O}_2$ ). This is followed by the HRP-catalyzed oxidation of ABTS which linearly correlates to the concentration of  $\text{H}_2\text{O}_2$ . The emergence of oxidized ABTS is indicated by the evolution of a green color, which is quantified by the decrease of the detected probe beam intensity  $I$  (Eq. (1)) of a standard laser diode (Laserdiode, 2004) emitting at  $\lambda_{\text{peak}} = 650 \text{ nm}$ .

On our centrifugal system, all steps of the glucose assay are implemented by a frequency protocol  $\nu(t)$  (Fig. 3(A)). After the uptake of the sample and reagents with the disk at rest, the disk is spun at  $\nu = 20 \text{ Hz} > \nu_c \approx 10 \text{ Hz}$  to overcome the capillary burst-valves and transport the liquids into the detection cell. To enhance the diffusion-limited speed of the reaction by inertially induced advection, we frequently reverse the sense of rotation (trapezoidal acceleration ramp with  $\Delta\nu/\Delta t = 32 \text{ Hz/s}$ ,  $\nu_{\text{max}} = 8 \text{ Hz}$ , and 45 s processing time). This so-called “shake-mode” has proven to accelerate mixing in this particular layout from 6.5 minutes for mere diffusion, to 5 s (Grumann et al., 2005e).

The disk is then spun at  $\nu = 30 \text{ Hz}$  for 90 s to clear the cellular constituents of the blood, mainly red blood cells (RBCs) from the optical beam path (Fig. 3(B)). The RBCs would otherwise interfere with the optical detection. Our calculations reveal that RBCs with a specific density of  $\rho_{\text{RBC}} = 1.06 \text{ g/cm}^3$  are moved towards the outer perimeter of the disk ( $z$ -direction, Fig. 3(B)) with a velocity  $1.32 \cdot 10^{-4} \text{ m/s}$  confirmed by the experimentally obtained velocity  $u_{\text{RBC}} = 1.48 \cdot 10^{-4} \text{ m/s}$  of the shock interface between plasma and cellular constituents. Accordingly, the sedimentation process is completed and the optical beam path is cleared out within  $t_{\text{sedi}} = 90 \text{ s}$ . Finally, the initial glucose concentration  $c$  is determined during constant spinning at  $\nu = 8 \text{ Hz}$ .

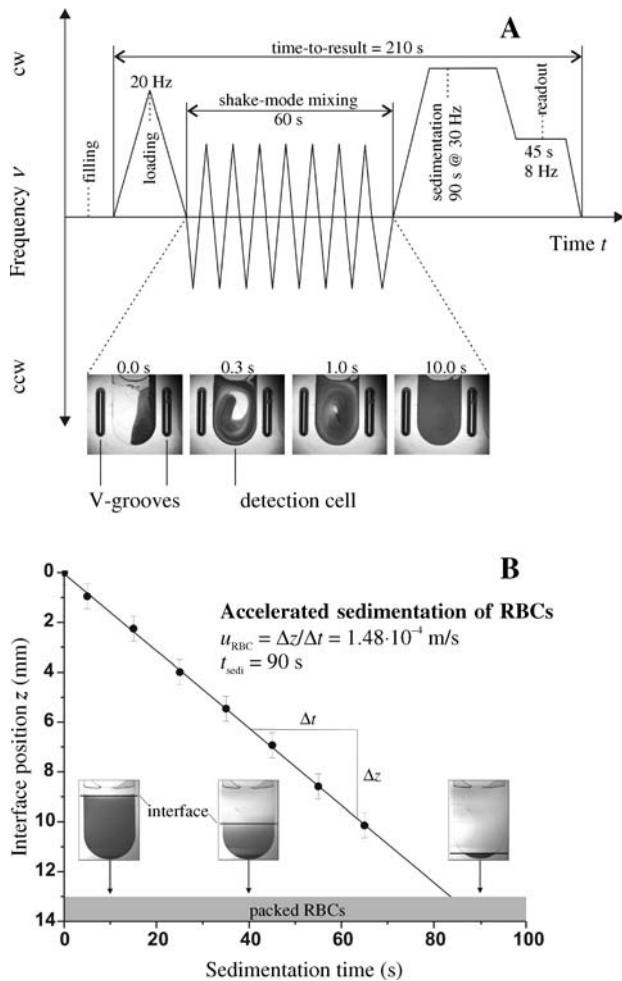


**Fig. 3** Frequency protocol  $\nu(t)$  to conduct a whole-blood assay within 210 s. (A) After the disk is placed on the spinning drive, the sample and reagents are loaded into their respective inlet reservoir. Next, the liquids are transported into the detection cell by means of the centrifugal force  $F_v$  at  $\nu = 20 \text{ Hz}$ . Mixing is completed within 5.1 s by frequently reversing the sense of rotation (“shake-mode”) (Grumann et al., 2005e). (B) To clear-out the optical beam path, this is followed by an accelerated sedimentation of cellular constituents, mainly RBCs of the whole blood sample by centrifugation at  $\nu = 30 \text{ Hz}$

### Enhancement of the sensor resolution

The predicted enhancement of the sensor performance (Eq. (1)) is validated by a series of experiments with a standard sample (Horse serum). We compared the on-disk concept of guiding an optical beam with a path length  $l_{\text{abs}}$  of 10 mm with a conventional perpendicular alignment configuration  $L_{\text{abs}} = 1 \text{ mm}$ . From Fig. 4, it turns out that, as expected, the slope  $\Delta A / \Delta c$  representing the resolution of the sensor scales with the ratio of the absorption lengths (Eq. (1)). In the TIR setup, the resolution is hence improved by a factor of 10.

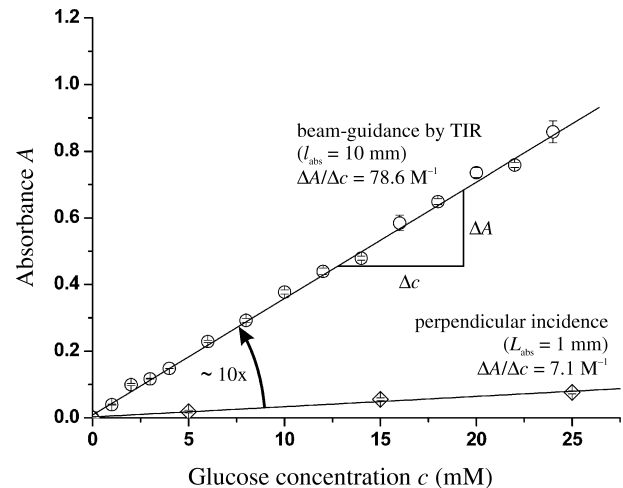


**Fig. 4** The slope of the characteristic absorption curve  $\Delta A / \Delta c$  which is a decisive impact factor for the resolution is improved by a factor of 10 compared to perpendicular incidence of the beam on the detection cell. The error bars of each data point represent the CV of 15 measurements

### Reduction of the measurement time

To shorten the measurement time as part of the total time-to-result of the assay, the increase of the absorbance  $A$  (Eq. (1)) is, in our approach, monitored during constant spinning for  $t_{\text{det}} = 45 \text{ s}$  and the saturation value  $A_{\infty}$  is extrapolated by a regression fit to the recorded data points (Fig. 5(A)). The obtained saturation values  $A_{\infty}$  at  $t_{\infty} = 120 \text{ s}$  are then plotted against the glucose concentrations used. With a correlation coefficient of  $R^2 = 0.9996$ , the experimental saturation values well comply with the linear scaling expected from the law of Beer-Lambert (Fig. 5(B)), (Eq. (1)).

### Internal calibrations

To run internal calibrations and to rule out noise effects, a second identical fluidic structure can be integrated which serves as a reference. Due to its finite spot size, the first V-groove evenly splits the probe beam into opposite directions. This way, one of the partial beams passes a reference cell of identical shape which is filled with a reference solution. The differential measurement allows to compensate fluctuations of the laser intensity. This has been verified with a standard sample (Horse serum) by deliberately induced changes of the laser output power of  $CV = 7.3\%$ , leading to a  $CV$  of 1.7% after compensation (data not shown).

### Glucose determination on human whole blood

A series of disk-based measurements are carried out with human whole blood at known glucose concentrations  $c$  (Fig. 6).

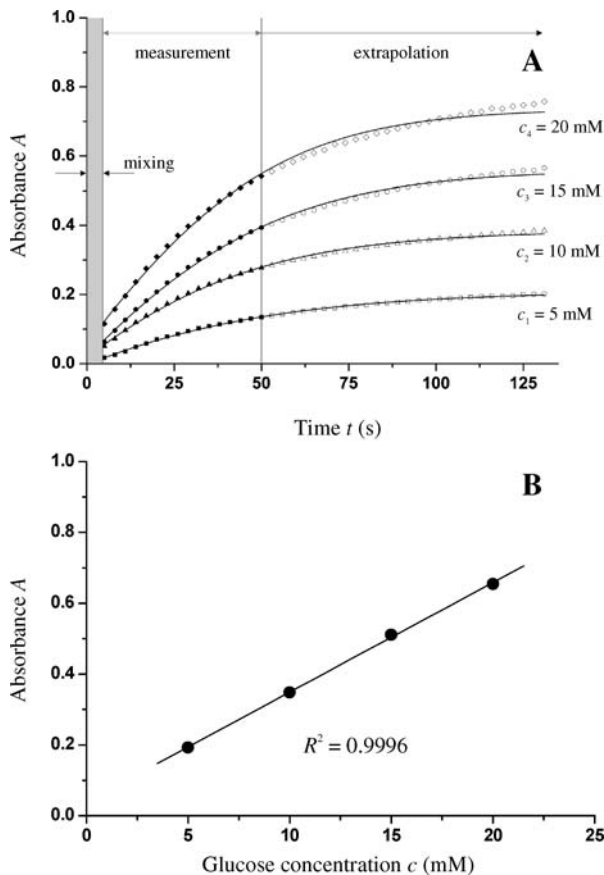


**Fig. 5** Real-time readout of the colorimetric assay. (A) The increase of the absorbance  $A$  of a fully processed standard sample (Horse serum) with known glucose concentrations  $c$  is recorded for  $t_{\text{det}} = 45$  s (filled symbols) and then extrapolated by a regression fit to its saturation value  $A_{\infty}$ . (B) The extrapolated values comply well with the measurements and the nominal values of  $c$  ( $R^2 = 0.9996$ ). This way, the readout time  $t_{\text{det}}$  can be reduced by 70 s

The recorded data-points display an absorption characteristics complying with the law of Beer-Lambert (Eq. (1)). In more detail, we obtain a  $CV$  of 4.0%, a lower limit of detection  $c_{\text{min}} = 200 \mu\text{M}$ , and a highly linear relation between the glucose concentration and the optical signal ( $R^2 = 0.997$ ).

In an additional experiment, we investigated the influence of the hematocrit  $HCT$  to the measured glucose. (The hematocrit  $HCT$  represents the fraction of the volume  $V_{\text{RBC}}$  containing the RBCs with respect to the total blood volume  $V_{\text{total}}$ ). By adding or removing plasma, the  $HCT$  was varied while maintaining a constant glucose concentration  $c$ . The so obtained reproducibility with a  $CV_{HCT}$  of 4.0% matches the  $CV$  of the previous experimental calibration curve (Fig. 6). This means that the influence of the  $HCT$  on the measured value of the glucose is negligible. Compared to conventional handheld devices for glucose measurement, with a rather large  $HCT$ -dependency (e.g., the Accu-Chek from Roche Diagnostics (Accu-Chek, 2004) with  $CV_{HCT} =$

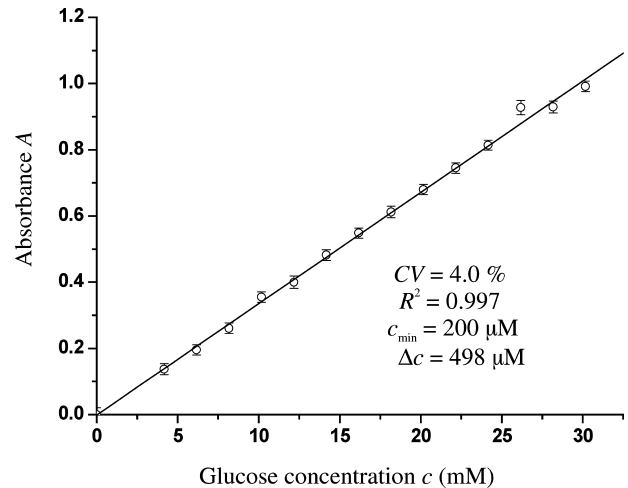


**Fig. 6** Results of glucose determination. Human whole blood as sample with an initial glucose concentration  $c = 3.8$  mM is spiked by adding glucose to expand concentrations beyond the physiological limits. With a  $CV$  of 4.0%, a lower limit of detection of  $c_{\text{min}} = 200 \mu\text{M}$ , and a linearity of  $R^2 = 0.997$ , our setup allows measurements with high accuracy

7.2%), the independence of the glucose measurement from the  $HCT$  is of particular benefit for emergency diagnostics where the  $HCT$  often displays large variations (Tang et al., 2000).

## Conclusions

We realized a novel optical method for sensitive readout of colorimetric assays in lab-on-a-chip systems by sizeable extension of the optical path length through the detection cell compared to perpendicular beam incidence onto the flat substrate. The optical beam-guidance is based on the total internal reflection at V-grooves which are monolithically incorporated on the polymer chip. The simple and rugged concept is successfully implemented in a modular setup comprising a laser diode, a spectrophotometer, and an exchangeable polymer disk which can readily be manufactured by standard polymer micromachining techniques. The centrifugal platform furthermore allows the integration of analytical process steps, e.g. mixing, an accelerated sedimentation of RBCs by centrifugation, as well as real-time measurements.

In a disk-based, colorimetric glucose-assay on human whole blood, the system shows excellent reproducibility ( $CV = 4.0\%$ ), an outstanding lower limit of detection ( $c_{\text{min}} = 200 \mu\text{M}$ ), and a high degree of linearity ( $R^2 = 0.997$ ) within a working range extending over nearly three orders of magnitude. This robust and cost-efficient approach can be readily adapted for enzyme-linked immunosorbent assays (ELISA). The rotational symmetry of the lab-on-a-disk concept permits

parallel screening and a real-time monitoring of several channels during spinning by only one spatially fixed detector.

## Acknowledgements

The authors thank the federal state of Baden-Württemberg (contract 24-720.431-1-7/2) for partial financial support of this project. Gerhard Jobst, Bernd Aatz, and the HSG-IMIT are acknowledged for their good cooperation.

## References

- ABTS (2,2'-Azino-bis(3-ethylbenzthiazoline-6-sulfonic acid),  $c_{\text{ABTS}} = 2 \text{ mM}$ ,  $V_{\text{ABTS}} = 66.7 \mu\text{l}$ , Sigma-Aldrich GmbH, Germany, www.sigmaaldrich.com, accessed 2005e.
- Accu-Chek, Roche Diagnostics, Switzerland, www.roche.com, accessed 2004.
- P. Auroux, D. Reyes, D. Iossifidis, and A. Manz, *Anal. Chem.* **74**, 2637–2652 (2002).
- I. Badr, R. Johnson, M. Madou, and L. Bachas, *Anal. Chem.* **74**, 5569–5575 (2002).
- Cyclic olefin copolymer (Topas<sup>®</sup>, www.ticona.com), accessed 2004.
- J. Ducreé and R. Zengerle, *FlowMap—Microfluidics roadmap for the life sciences* (Books on Demand GmbH: Norderstedt, Germany, ISBN 3-8334-0744-1, 2004), www.microfluidics-roadmap.com, accessed 2004.
- G. Ekstrand, C. Holmquist, A. Örléon, B. Hellmann, A. Larsson, and P. Andersson, (Proceedings of the  $\mu\text{TAS}$  2000 conference, edited by A. van den Berg, and P. Bergveld, Kluwer Academic Publisher, Dordrecht, NL, 2000), pp. 311–314.
- Examples in clinical diagnostics: Careside Analyzer<sup>®</sup>, Careside Inc, USA, www.careside.com; Biosite<sup>®</sup> Biosite Inc., France, www.biosite.com; Pelikan Sun<sup>TM</sup> of Pelikan Technologies Inc., USA, www.pelikantechnologies.com; Chempaq Analyzer, Chempaq A/S, Denmark, www.chempaq.com; i-STAT Portable Clinical Analyzer, i-STAT Corp., USA, www.istat.com, (all URLs accessed 2004).
- Fiber Collimation Package F220SMA-A, NA = 0.25, D = 5 mm, www.thorlabs.com
- GOD (glucose oxidase),  $c_{\text{GOD}} = 40 \text{ units/ml}$ ,  $V_{\text{GOD}} = 1.3 \mu\text{l}$ , Biozyme Laboratories, UK, www.biozyme.com, accessed 2005.
- M. Grumann, M. Dube, T. Brefka, J. Steigert, L. Riegger, T. Brenner, K. Mittmann, R. Zengerle, and J. Ducreé, (Proc. Transducers 05 – The 13<sup>th</sup> conference on Solid State Sensors, Actuators and Microsystems, Seoul, Korea, June 2005c), pp. 1106–1109.
- M. Grumann, A. Geipel, L. Riegger, R. Zengerle, and J. Ducreé, *Lab Chip* **5**, 560–565 (2005e).
- M. Grumann, I. Moser, J. Steigert, L. Riegger, A. Geipel, C. Kohn, G. Urban, R. Zengerle, and J. Ducreé. Piscataway, NJ: Proc. MEMS 2005, IEEE, USA, (2005a), pp. 108–111.
- M. Grumann, L. Riegger, A. Geipel, R. Zengerle, and J. Ducreé, *Vorrichtung und Verfahren zur Umlenkung eines Lichtstrahls*, Patent application January 21, 2005b, Document number DE 10 2005 002 348.
- M. Grumann, L. Riegger, T. Nann, J. Riegler, O. Ehlert, K. Mittenbühler, G. Urban, L. Pastewka, T. Brenner, R. Zengerle, and J. Ducreé, *Proc. Transducers 05 – The 13<sup>th</sup> Conference on Solid State Sensors* (Actuators and Microsystems, Seoul, Korea, June 2005d), pp. 1114–1117.
- Horse serum with an initial glucose concentration  $c_0$  of 4.0 mM. Spiking of the sample was achieved by adding glucose, dilution by adding PBS-buffer.
- HRP (horseradish peroxidase),  $c_{\text{HRP}} = 4 \text{ units/ml}$ ,  $V_{\text{HRP}} = 1.3 \mu\text{l}$ , Sigma-Aldrich GmbH, Germany www.sigmaaldrich.com, accessed 2005.
- S. Lai, S. Wang, J. Luo, L. Lee, S. Yang, and M. Madou *Anal. Chem.* **76**, 1832–1837 (2004).
- Laserdiode LDM650/1LJ, fixfocus,  $\lambda_{\text{peak}} = 650 \text{ nm}$ , 1 mW, Roithner Lasertechnik, Austria, www.roithner-laser.com, accessed 2004.
- Z. Liang, N. Chiem, G. Ocvirk, T. Tang, K. Fluri, and D. Harrison *Anal. Chem.* **68**, 1040–1046 (1996).
- M. Madou and G. Kellogg. (Proceedings of SPIE, vol. 3259, 1998, 80–93, 1998).
- M. Madou, Y. Lu, S. Lai, J. Lee, and S. Daunert, (Proceedings of the  $\mu\text{TAS}$  2000 conference, edited by A. van den Berg, P. Bergveld, P. Kluwer Academic Publisher, Dordrecht, NL, 2000), pp. 565–570.
- M. McNeely, M. Spute, N. Tusneem, and A. Oliphant, (Proc. SPIE – Microfluidic Devices and Systems II, 1999, edited by C. Ahn, and A. Frazier, A. (B.1.2, B.6), 3877, 1999), pp. 210–220.
- R. Oosterbroek and A. van den Berg, *Lab-on-a-Chip: Miniaturized systems for (bio)chemical analysis and synthesis* (Elsevier Science, Amsterdam, NL, 2003).
- N. Petersen, K. Mogensen, and J. Kutter, *Electrophoresis* **23**, 3528–3536 (2002).
- Phosphate buffered saline – PBS (0.1 M phosphate, 0.1 M NaCl, pH = 7.4).
- D. Reyes, D. Iossifidis, P. Auroux, and A. Manz, *Anal. Chem.* **74**, 2623–2636 (2002).
- J. Roulet, R. Völkel, H. Herzig, E. Verpoorte, and N. de Rooij, *Journal of Microelectromechanical Systems* **10**, 482–491 (2001).
- T. Schulte, R. Bardell, and P. Weigl, *Clinica Chimica Acta* **321**, 1–10 (2002).
- S. Sia, V. Linder, B. Parviz, A. Siegel, and G. Whitesides, *Angew. Chem. Int.* **43**, 498–502 (2004).
- B. Splawn, F. Lytle, and *Anal. Bioanal. Chem.* **373**, 519–525 (2002).
- Z. Tang, J. Lee, R. Louie, G. Kost, *Archives of Pathology and Laboratory Medicine* **124**, 1135–1140 (2000).
- UV/VIS Microspectrometer, Boehringer Ingelheim MicroParts AG, Germany, www.microparts.de, accessed 2004.
- E. Verpoorte, *Lab Chip* **3**, 42N–52N (2003).
- E. Verpoorte, A. Manz, H. Lüdi, A. Bruno, F. Maystre, B. Krattinger, H. Widmer, B. van der Schoot, and N. de Rooij, *Sensors and Actuators B* **6**, 66–70 (1992).
- T. Vilknér, D. Janasek, and A. Manz, *Anal. Chem.* **76**, 3373–3386 (2004).
- D. Walt, *Science* **287** (5452), 451–452 (2000).
- J. Zeng, D. Banerjee, M. Deshpande, J. Gilbert, D. Duffy, and G. Kellogg, (Proc.  $\mu\text{TAS}$  2000 conference, Kluwer Academic Publisher, Dordrecht, NL, 2000), pp. 579–582.